Modeling and Measurement of Shear Stress for a Slug Flow Inside a Capillary

S. Laborie and C. Cabassud
Laboratoire d'Ingénierie des Procédés de l'Environnement, Institut National des Sciences Appliquées, 31077 Toulouse Cédex, France

DOI 10.1002/aic.10382
Published online March 3, 2005 in Wiley InterScience (www.interscience.wiley.com).

The aim of the present study is to characterize wall shear stresses generated by a gas–liquid two-phase flow inside a capillary tube. In this case the flow is a slug flow. Two different approaches were used. The first one constituted a calculation of the shear stresses by a two-phase model in which some parameters characteristics of the flow were introduced. These parameters had been determined experimentally in a previous study. The second approach constituted a direct and local measurement of wall shear stresses by an electrochemical method. The shear stresses near liquid and gas slugs were obtained for different operating conditions. Moreover, a calculation of the liquid film thickness around the gas slugs demonstrated that this thickness does not depend on gas velocity. © 2005 American Institute of Chemical Engineers *AIChE J,* 51: 1104–1115, 2005
Keywords: gas–liquid two-phase flow, slug flow, wall shear stresses, modeling, electrochemical measurement

Introduction

Ultrafiltration by hollow fibers is now widely developed for drinking water supplies. Many plants are in operation in the world. The principal limitation of this process lies in the flux decline associated with the formation of a particle deposit on the membrane wall.

During the last few years, the use of gas in membrane processes has been the focus of increasingly investigations, either to limit the particle deposit or to eliminate it after its formation on the membrane wall.

In the latter case, gas is injected periodically during the washing step, such as in an ultrafiltration membrane.[1,2]

The other possibility is to inject the gas together with the feed (water and particles), to generate a two-phase flow that tends to limit the particle deposit resistance and thus to enhance the water flux through the membranes. Different studies have shown the efficiency of this gas–liquid two-phase flow, in tubular membranes,[3-5] in hollow fibers,[6-8] and also in flat-sheet nanofiltration membranes.[9]

In many cases, mass transfer is supposed to be dependent on wall shear stresses near the membrane surface and also on particle–membrane and particle–particle interactions. Many recent studies[5,10-12] propose to establish a link between wall shear stresses and flux enhancement.

Along the lines of that idea, it was of interest to characterize the wall shear stresses induced by the air slug flow inside hollow fibers.

Experimental and theoretical characterization of this type of flow has already been performed in large-diameter pipes.[13,14] In the present study, the investigative focus is on capillary tubes with an inner diameter of 1×10^{-3} m. Two complementary approaches will be used and discussed. The first one uses a calculation of the shear stress from some slug characteristics, such as the gas slug velocity and the slug frequency, which were determined experimentally in a previous study.[15] The second one uses a direct measurement of the shear stresses using an electrochemical method. Because the determination was not possible inside the fibers themselves, experiments were carried out in glass-pipe capillaries having the same inner diameter as that of the fibers.

Correspondence concerning this article should be addressed to C. Cabassud at corinne.cabassud@insa-toulouse.fr.

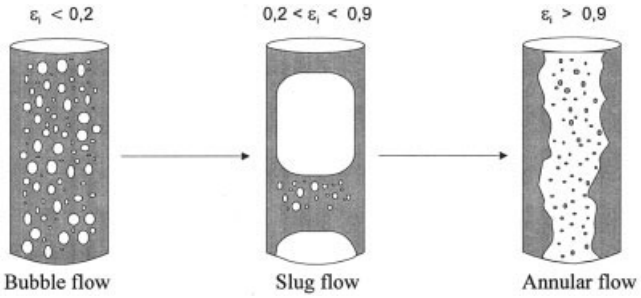

Figure 1. Gas–liquid two-phase flow patterns inside a pipe.

The aim of the work described herein is to describe the two approaches and their limitations and to compare the results.

Description of the Two-Phase Flow Inside Capillaries

Three different flow patterns can be observed inside pipes (see Figure 1): a bubble flow, a slug flow, and an annular flow, depending on the value of the air injection ratio ε_i defined as

$$\varepsilon_i = \frac{U_{\text{Gas}}}{U_{\text{Gas}} + U_{\text{Liq}}} \tag{1}$$

where U_{Gas} and U_{Liq} are, respectively, the superficial gas velocity and the superficial liquid velocity, both velocities being calculated as if each phase were circulating separately in the tube.

In a previous study,[15] experiments elucidated a great deal of information about gas–liquid two-phase flow inside pipes of small diameter ($D = 1$, 2, 3, and 4×10^{-3} m).

In a capillary of 1×10^{-3}-m inner diameter, the flow pattern has been demonstrated to be a slug flow (see Figure 2) for $0 < U_{\text{Gas}} < 1$ m s^{-1} and $0.25 < U_{\text{Liq}} < 0.9$ m s^{-1}. For this range of velocity values, even for $\varepsilon_i < 0.20$, a slug flow is always observed.

The liquid slug is shown to contain no small dispersed bubbles, contrary to what is observed in pipes of larger diameter. The air slug is rather cylindrical and surrounded by a liquid film. The thickness of this film is not measurable by visualization.

The liquid flow induces two alternate shear stresses near the membrane wall: τ_{LLiq} is generated by the liquid slug and τ_{LGas} is generated by the liquid film near the gas slug.

Different parameters of the flow were previously characterized[15] and will be introduced in the following modeling.

Modeling of Wall Shear Stresses

The first step of this study consists in calculating the wall shear stresses using a two-phase slug flow model, previously developed by Fabre and Liné.[16]

In a fixed point of the tube, the flow (liquid and gas slugs) is intermittent, and thus nonstationary, whereas the conditions (inlet flow rates and outlet pressure) are stationary. To treat the problem, the concept of unit cell has been developed, which considers the flow as a sequence of cells being periodic with both space and time. This concept is based on two assumptions: (1) a frame of a given velocity (of the gas slugs, V_s) exists, in which the flow is almost steady; and (2) in this frame the flow in bubbles and liquid slugs is fully developed. The problem becomes stationary.

Some global parameters can be calculated from known experimentally determined parameters.

- The gas and liquid superficial velocities, expressed as

$$U_{\text{Gas}} = \frac{Q_{\text{Gas}}}{\pi r^2} \tag{2}$$

$$U_{\text{Liq}} = \frac{Q_{\text{Liq}}}{\pi r^2} \tag{3}$$

where r is the capillary radius.

- The gas and liquid holdup, defined as

$$R_{\text{G}} = \frac{V^{\text{G}}}{V} \tag{4}$$

$$R_{\text{L}} = 1 - R_{\text{G}} \tag{5}$$

- The gas and liquid fluxes, expressed as

$$\Phi_{\text{G}} = R_{\text{G}} V_s - U_{\text{Gas}} \tag{6}$$

$$\Phi_{\text{L}} = R_{\text{L}} V_s - U_{\text{Liq}} \tag{7}$$

- Moreover, wall shear stresses are generally defined by analogy with the one-phase flow as

$$\tau = \frac{1}{2} \rho_{\text{L}} f U_{\text{L}}^2 \tag{8}$$

- The wall shear stress near the liquid slugs, given by

$$\tau_{\text{LLiq}} = \frac{1}{2} \rho_{\text{L}} f_{\text{Liq}} U_{\text{LLiq}}^2 \tag{9}$$

- The wall shear stress near the air slugs, expressed as

$$\tau_{\text{LGas}} = \frac{1}{2} \rho_{\text{L}} f_{\text{Gas}} U_{\text{LGas}}^2 \tag{10}$$

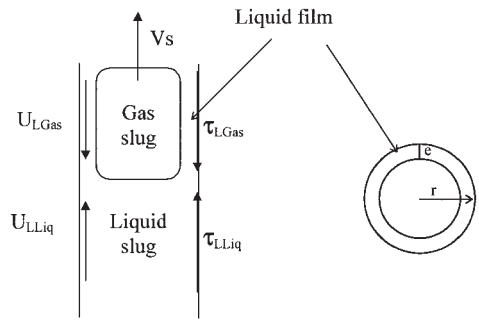

Figure 2. Slug flow inside a capillary.

Table 1. Equations Used for Modeling

Near the Liquid Slugs		Near the Gas Slugs	
$R_{LLiq} = 1$	(13)	$R_{LGas} = \frac{\pi r^2 - \pi(r-e)^2}{\pi r^2} = \frac{2e}{r}$	(18)
$U_{LLiq} = (1 - R_L)V_s + U_{Liq} = U_{Gas} + U_{Liq}$	(14)	$U_{LGas} = \frac{-\Phi_L}{R_{LGas}} + V_s$	(19)
$Re_{Liq} = \frac{U_{LLiq} D_{Liq} \rho_L}{\mu_L}$	(15)	$Re_{Gas} = \frac{U_{LGas} D_{Gas} \rho_L}{\mu_L}$	(20)
$D_{Liq} = 2r$	(16)	$D_{Gas} = 4e$	(21)
$f_{Liq} = \frac{16}{Re_{Liq}}$	(17)	$f_{Gas} = \frac{16}{Re_{Gas}}$	(22)

To calculate the different model parameters, the gas slug velocity V_s is required. In a previous study[15] V_s was determined by experiments of slug flow inside capillaries and it was demonstrated that V_s can be expressed as a function of the mean flow velocity U_m ($U_m = U_{Liq} + U_{Gas}$)

$$V_s = C_0 U_m \tag{11}$$

The parameter C_0 depends on the characteristics of the fluid and the inner diameter. In the case of air slugs inside water at 25°C and in a capillary of 1×10^{-3}-m inner diameter, C_0 is equal to 1.24. This relationship was used in this model.

The problem can then be treated in two separated parts:

(1) Near the liquid slugs: terms will include an index noted by the subscript Liq

(2) Near the gas slugs: terms will include an index noted by the subscript Gas

The index subscript L concerns the liquid phase and G, the gas phase, whatever the slug is.

The assumptions taken into account for the modeling are:

(1) The flow is laminar and the friction factor near the gas and liquid slugs can be calculated by

$$f = \frac{16}{Re} \tag{12}$$

The range of superficial velocities (in m s^{-1}) are $0.25 < U_{Liq} < 0.9$ and $0 < U_{Gas} < 1$, which corresponds to a maximum for the mean Reynolds number of 1900 (for a capillary diameter of 1 mm). Although the mean flow velocity in the liquid slug corresponds globally to laminar flow, locally, between two gas slugs, there may be some recirculations and higher local velocities, resulting in some cases of laminar flow that are not fully developed. However, for all calculations, the flow will be considered as laminar.

(2) The liquid slugs do not contain any gas ($R_{GLiq} = 0$).

(3) The gas flux between air and liquid slugs is null ($\Phi_G = 0$ and $R_G = U_{Gas}/V_s$).

The two last assumptions correspond to experimental observations.[15]

Considering these assumptions, equations that permit calculation of the parameters in each phase (Eqs. 13–22) are presented in Table 1. The system contains 19 equations and 20 unknowns. To calculate both of the wall shear stresses, the value of the film thickness around the slug e is needed (see Figure 2).

Different methods were found in the literature to estimate this value.

Fairbrother and Stubbs[17] calculated the value of e from direct measurements of liquid backflow in capillary tubes and established a simple empirical relationship for sufficiently long ($>3r$) moving bubbles

$$e = \frac{r}{2}\sqrt{\frac{V_s \mu_L}{\sigma_L}} \tag{23}$$

The main assumption is that the film around the moving bubble was at rest, so that the mean back velocity of the liquid film was V_s.

For a bubble of known length released in a tube containing moving liquid, Marchessault and Mason[18] derived the film thickness from the measurement of the electrical resistance of the tube. They found that the film grew thicker as V_s increases and proposed a relationship between the two parameters

$$e = \alpha'(-\beta' + \sqrt{V_s}) \tag{24}$$

where α' and β' are positives and depend on the liquid used and on the hydrodynamic conditions. In the case of water, at 25.5°C, and for a slug of 0.87 cm length inside a capillary of 1.54-mm inner diameter, the values given for α' and β' are, respectively, 8.6×10^{-4} (cm s)$^{0.5}$ and 0.10 (cm s^{-1})$^{0.5}$. Values of e are then included between 172 and 516 μm (for a slug velocity between 0.09 and 0.49 cm s^{-1}).

Bretherton[19] proposed an analytical approach to describe the film thickness, obtained by invoking the "lubrication " approximation, that is, by considering the flow quasi-unidirectional in the thin-film region. With a reasonable degree of rigor, Bretherton demonstrates that the "lubrication " approximation was valid and gave a unique analytical solution for the layer thickness, in the case of a nonmoving continuous phase and assuming a small value of e/r (which value was not specified in the text)

$$\frac{e}{r} = 0.643(3Ca)^{2/3} \tag{25}$$

where Ca is the capillary number

$$Ca = \left(\frac{\mu_L V_s}{\sigma_L}\right) \tag{26}$$

Schwartz et al.[20] also studied the average thickness of the wetting film left behind during the slow passage of an air bubble in a water-filled capillary tube. A dimensionless number, the parameter W, has been characterized. The amount V_sW represents the difference between the average gas slug velocity V_s and the average mean flow velocity U_m in the tube

$$W = \frac{V_s - U_m}{V_s} \tag{27}$$

W was experimentally obtained. It can be related to the film thickness e by

$$W = \frac{2e}{r} \tag{28}$$

For bubbles of length many times the radius, the ratio of film thickness to tube radius was found to be a function of the capillary number only. For bubbles of length $\lesssim 20$ tube radii, good agreement with the Bretherton predictions was obtained.

At the end of this literature study, we decided to adopt the Bretherton equation, based on an analytical approach, to obtain an estimation of the film thickness to calculate the wall shear stress near the gas slugs.

The validity of our modeling thus relies on the use of the Bretherton equation.

Including the Bretherton equation, the system contains 20 equations (2–7, 9–11, 13–22, 25) and 20 unknowns (U_{Gas}, U_{Liq}, Φ_G, R_G, V_s, Φ_L, R_L, R_{LLiq}, U_{LLiq}, Re_{Liq}, D_{Liq}, f_{Liq}, τ_{LLiq}, R_{LGas}, U_{LGas}, e, Re_{Gas}, D_{Gas}, f_{Gas}, τ_{LGas}). The problem can then be solved.

The model can be used for a first simulation of both shear stress near liquid slugs and shear stress near gas slugs. It can also enable a first prediction of the tendencies in the variation of the two shear stresses with operating parameters such as superficial velocities and capillary inner diameter.

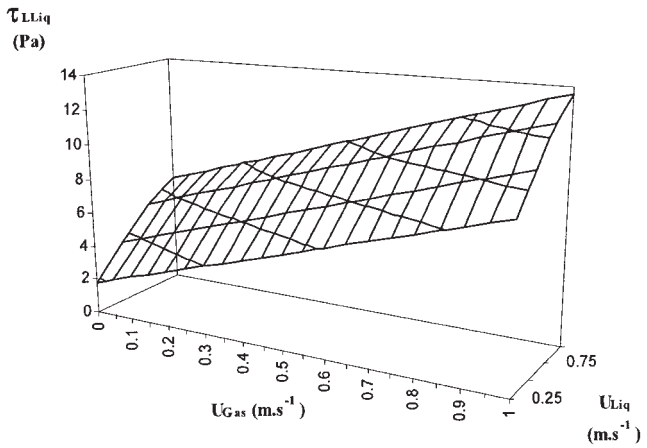

Figure 3. Wall shear stress near liquid slugs vs. U_{Liq} and U_{Gas}.

$D = 1 \times 10^{-3}$ m.

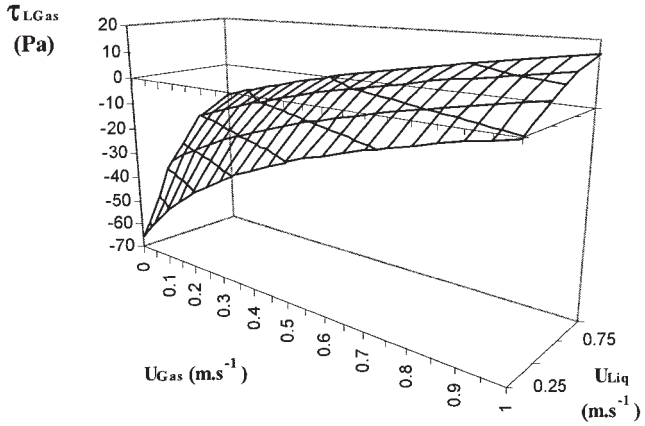

Figure 4. Wall shear stress near gas slugs vs. U_{Liq} and U_{Gas}.

$D = 1 \times 10^{-3}$ m.

Variation of computed wall shear stresses with superficial velocities

Figure 3 represents the variation of the wall shear stress near liquid slugs vs. U_{Liq} and U_{Gas}.

Without gas, for some liquid velocities usually used in drinking water production, the shear stress near the wall varies between 2 and 8 Pa, in a 1×10^{-3}-m inner diameter capillary. This shear stress increases when gas is injected, and also increases when values of U_{Liq} and U_{Gas} are higher. This result is quite logical because τ_{LLiq} is proportional to the mean velocity $U_m = U_{Liq} + U_{Gas}$ (see Eqs. 9 and 14–17).

Concerning the wall shear stress near gas slugs (Figure 4), for low values of superficial velocities, the calculated value of τ_{LGas} is negative, the liquid film around the gas slugs thus might flow down, in the direction opposite to that of the main flow. The absolute value of τ_{LGas} is then high. When U_{Gas} increases, this absolute value decreases and τ_{LGas} becomes positive for a limit value of U_{Gas}, which is lower when U_{Liq} is higher. Beyond this limit value, the wall shear stress near air slugs is positive, whatever U_{Gas} is, and increases with U_{Liq}.

For $U_{Liq} = 0.9$ m s^{-1}, the wall shear stress near gas slugs is equal to -3.6, 4, 10.4, and 13.7 Pa, respectively, for $U_{Gas} =$ 0.25, 0.5, 0.75, and 0.9 m s^{-1}.

It must be pointed out that in the 1×10^{-3}-m inner diameter capillary, the modeling leads to a limit value of τ_{LGas} (-65 Pa), when U_{Gas} tends to 0, which has no physical significance. In fact, the wall shear stress should be $\tau_{LGas} = 0$ or $\tau_{LGas,} = \tau_{LLiq}$ when U_{Gas} tends to 0.

Influence of the capillary inner diameter on computed wall shear stresses

For the same mean velocity and the same liquid viscosity and temperature, the wall shear stress near liquid slugs is inversely proportional to the tube diameter (Eqs. 9 and 14–17) with or without gas. τ_{LLiq} decreases when D increases (Figure 5).

Near the gas slugs (Figure 6), the wall shear stress is negative for $D = 1 \times 10^{-3}$ m until $U_{Gas} = 0.8$ m s^{-1}. For $D \geq 2 \times 10^{-3}$ m, τ_{LGas} is always positive and decreases when D increases.

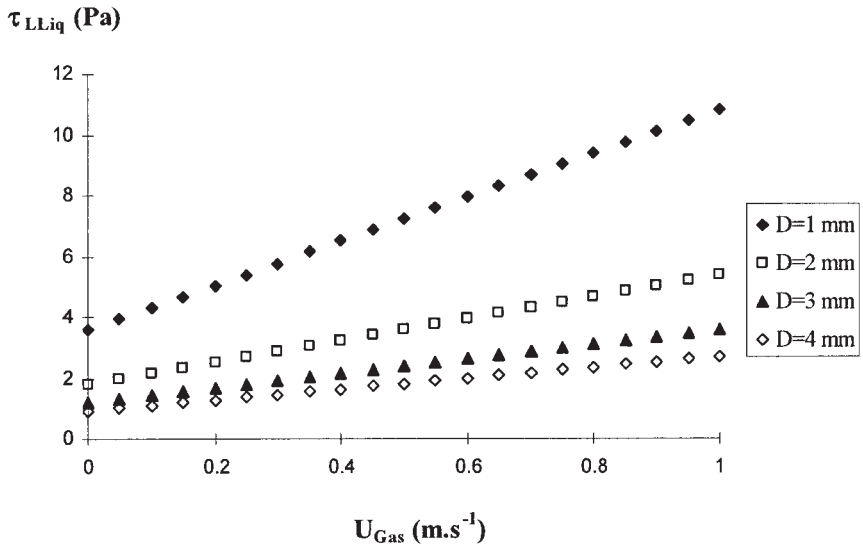

Figure 5. Wall shear stress near liquid slugs vs. U_m for different capillary inner diameters.

$U_{Liq} = 0.5$ m s^{-1}.

The modeling gives only a first approach of the variation of wall shear stresses with operating conditions. Indeed, some results are difficult to explain from a physical perspective. For that reason, it was decided to perform an experimental determination of wall shear stresses.

Measurement of Wall Shear Stresses

As a complementary approach a direct local measurement of shear stresses was performed in the 1-mm-diameter capillary without mass transfer through the wall. The experimental method was based on an electrochemical determination.

In the field of chemical engineering, an electrochemical method was developed in the 1960s to measure mass transfer coefficients. The first studies were led by Reiss and Hanratty.[21,22] An electrochemical reaction was operated at a microprobe placed on a pipe wall in contact with a one-phase flow. This method enabled measurement of local mass transfer coefficients, which can be related to velocities in the vicinity of the probe.

Cognet[23] applied this method to the study of the Couette flow between two coaxial cylinders.

Koeck[24] and Cognet et al.[25] were the first investigators to apply this methodology to the measurement of the wall shear rate generated by a gas–liquid two-phase flow inside a duct. The results obtained by this measurement method were in good agreement with the momentum balance equation because the error was $<5\%$.

In the case of membrane applications, recent studies have been carried out using this electrochemical method to determine wall shear stresses for a one-phase flow. Galier et al.[26]

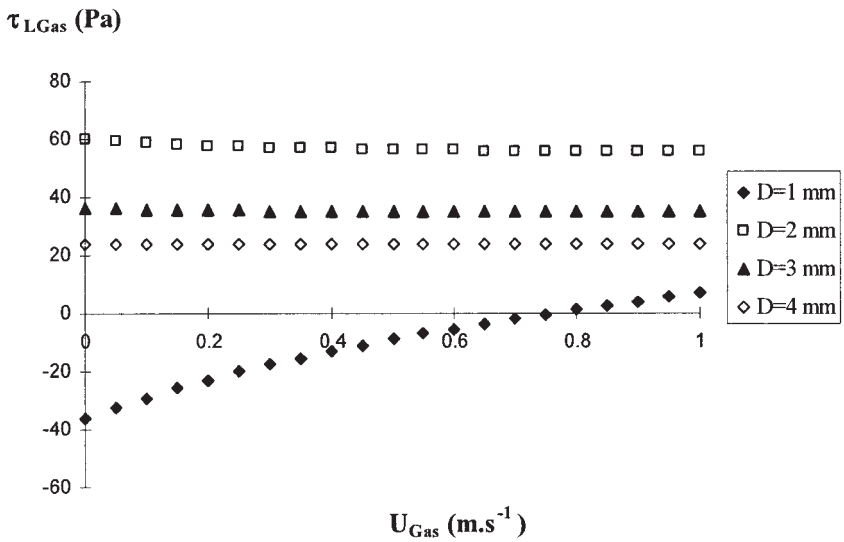

Figure 6. Wall shear stress near gas slugs vs. U_{Gas} for different capillary inner diameters.

$U_{Liq} = 0.5$ m s^{-1}.

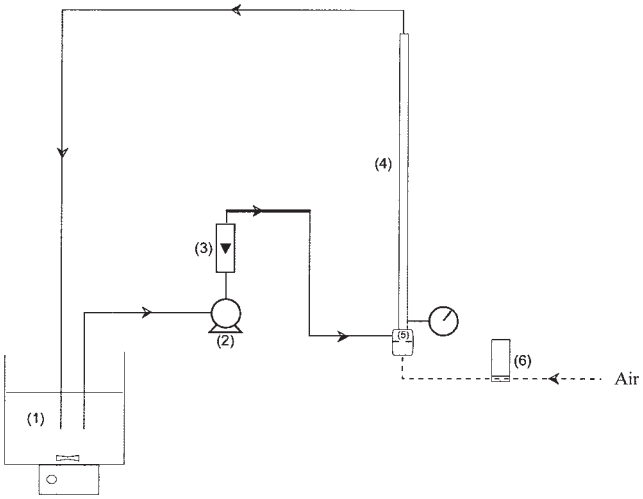

Figure 7. Experimental apparatus for electrochemical measurements.

applied this technique to the measurement of shear stresses generated in a nonporous helical module and Gaucher et al.[27] determined the thickness and the porosity of a deposit during ultrafiltration experiments in a plane membrane.

This brief bibliography review shows the wide application field of this electrochemical method, which has today become useful in various areas. Previous studies concerning gas slug flows were carried out only in large pipes (inner diameter of a few centimeters).

In the case of our study, the aim was to apply this electrochemical method to the measurement of wall shear stresses generated inside capillary tubes whose inner diameter is only a few millimeters, which induced far more important technological difficulties.

Principle of the electrochemical method

The measurement leads on an apparatus include three probes (a cathode, an anode, and a reference probe) placed in the flow inside a nonporous glassy capillary tube of 1 mm inner diameter.

A potential difference between the work probe (cathode) and the reference probe is kept constant by a potentiostat to a certain value E, different from the balance potential of the redox couple.

A reaction takes place at the cathode, inducing a concentration gradient and then a mass transfer, which involves the establishment of an electric current i between the cathode and the anode. For a correctly chosen value of E, the obtained current is a diffusion limit current (constant with time) and is a function of hydrodynamics and more particularly of the velocity gradient S.

Experimental procedure

Experimental Apparatus. A schematic of the experimental apparatus is shown in Figure 7. Experiments were carried out in a glass capillary (4) placed vertically. The inner diameter was 1×10^{-3} m and the length about 1.2 m. The electrolyte (1) was injected inside the capillary by a Volumax volumetric pump (2) (range of flow rate: 0–10 L h^{-1}). Air was injected at the bottom of the capillary and the air flow rate was measured by a Brooks mass flow meter (6) (0–20 nL h^{-1}); the air injector was a flexible porous membrane (5). The fluid velocities (in m s^{-1}) ranged between 0.3 and 1 for the liquid and 0.05 and 1.3 for the gas.

All electrochemical measurements were carried out thanks to the three-probe assembly connected to an electrochemical system (Voltalab™32 from Radiometer Copenhagen), including a potentiostat (potential range: ±8V) linked to a computer (Voltamaster 2® software). A schematic of the three-probe assembly is shown in Figure 8.

Work Probe. The cathode (work probe) consisted of a gold thread of 250 μm diameter. It was stuck normally to the flow axis and tangentially to the inner surface of the capillary (see Figure 8). The probe surface must be perfectly smooth and not enter inside the tube so as not to disturb the flow.

Because the probe is of small dimension, it allows the measurement of only a local velocity gradient S, which can be related to local wall shear stress. It is important to note that only the absolute value of the wall shear stress can be obtained with this measurement system. The sign of the shear stress cannot be known.

Electrolyte. The electrolyte used in experiments was an aqueous solution of potassium ferri/ferrocyanure, to which KCl was added to limit the mass transfer of the species by migration.

The reactions involved are the following:

- At the cathode

$$[Fe(CN)_6]^{3-} + e^- \rightarrow [Fe(CN)_6]^{4-}$$

- At the anode

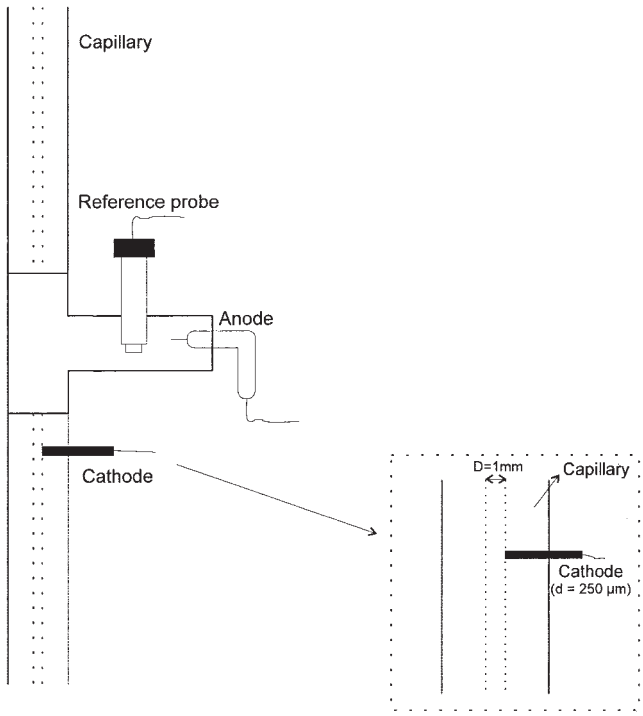

Figure 8. Three-probe circuit.

$$[Fe(CN)_6]^{4-} \rightarrow [Fe(CN)_6]^{3-} + e^-$$

The concentrations used were $[Fe(CN)_6]^{3-} = 3$ mol m^{-3}; $[Fe(CN)_6]^{4-} = 6$ mol m^{-3} and [KCl] = N/3.

Electrochemical Methods. The diffusion limit current was measured by chronoamperometry (that is, a measurement of the current vs. time, for an applied voltage of −300 mV, for 100 s). The average value of i was used in Eq. 29.

Relationship between Limit Current Intensity and Shear Stresses. In the case of a circular probe, Storck and Coeuret[28] proposed a relationship between i, S, and properties of both the work probe and the solution.

$$i = \frac{0.863nFC_1D_f^{2/3}S^{1/3}\pi d^2}{d^{1/3}4} = KC_1S^{1/3} \qquad (29)$$

From the direct measurement of i, S can be calculated and, for a Newtonian fluid with dynamic viscosity μ_L, the wall shear stress can be expressed as

$$\tau = S\mu_L \qquad (30)$$

Standardization with a one-phase flow

Equation 29 takes into account the diameter of the work probe, although because of the way the probe was built, the exact probe diameter in contact with the fluid was unknown.

The constant term K is a characteristic of the probe and of the solute used. K can be determined using calibration tests.

Indeed, for a one-phase water flow, a theoretical value of the wall shear stress can be calculated from the relationship between the shear stress τ and the liquid velocity U_L, in the case of a laminar flow

$$\tau_{theo} = \frac{8\mu_L U_L}{D} \qquad (31)$$

The standardization consists in minimizing the gap between theoretical and experimental values of the shear stress in a one-phase flow by adjusting the value of K.

A laminar one-phase flow was generated in the capillary, at different liquid velocities. For each value of the velocity, the theoretical value was calculated (Eq. 31) and the limit current was also measured. It was verified that the measured value of i is proportional to $S^{1/3}$, so Eq. 29 can be applied. K was determined, which allowed an estimation of the probe diameter of 262 μm. This value is very close to the diameter given by the provider (250 μm) for the thread used to manufacture the probe.

Figure 9 shows the variation of τ_{exp} vs. τ_{theo}. The mean gap to the bisecting line is <10%.

Measurement of wall shear stresses generated by a two-phase flow in a capillary

Effect of a Gas Slug on the Electrical Signal. The effect of a gas slug on the electrical signal was determined using low gas velocities. Figure 10 shows an example of the measured electrical signal when a two-phase flow is generated. Each peak of current corresponds to a passing gas slug that has been confirmed by a simultaneous visualization of the flow. The observed baseline corresponds to a passing liquid slug.

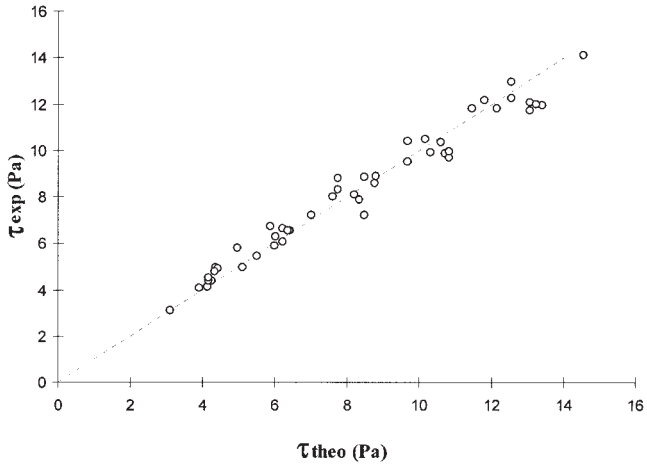

Figure 9. Experimental wall shear stress vs. theoretical value (one-phase flow).

The value of the intensity corresponding to a passing gas slug is called I_{Gas} and the value of the current corresponding to a passing liquid slug is called I_{Liq}. These values were always negative because the measurement was realized for a reaction operated as an electrochemical reduction. The use of the absolute values of I_{Gas} and I_{Liq} enabled us to achieve values of experimental wall shear stress, respectively, for the gas slugs (τ_{LGas}) and for the liquid slugs (τ_{LLiq}). For fixed experimental conditions (U_{Gas}, U_{Liq}), the value of current measured for gas and liquid slugs may vary because of the dispersion of measurements. The value taken for shear stress calculations is an arithmetic mean value, calculated from about 200 measurements of I. The experimental error on the shear stress calculation is between 15 and 25%, depending on operating conditions.

Wall Shear Stress Measurement in Liquid Slugs: First Validation of the Experimental Method. Experimental values of τ_{LLiq} can be compared to those calculated by Eq. 8 using U_m instead of U_L. Indeed, the liquid velocity near a liquid slug can be expressed as the mean velocity U_m, which is the sum of the liquid and of the gas velocities, each velocity being calculated as if each phase were circulating alone (Eq. 14). Figure 11 represents the variation of the measured wall shear stress as a function of the theoretical value.

It appears that experimental and theoretical values of τ_{LLiq} are very close. The gap from the bisecting line is <5%, except for 5 points, in the low shear stress region, corresponding to the lowest liquid velocity ($U_{Liq} = 0.32$ m s^{-1}). For this velocity, experimental error is the highest (lower slug frequency, less experimental points).

Taking into account experimental errors, this measurement of the wall shear stress near the liquid slugs thus allows validation of the electrochemical method.

Validation of the Method by Gas Slug Frequency Measurement. The variation of the intensity vs. time during a two-phase flow also enabled us to obtain the gas slug frequency. On the other hand, this parameter has already been measured in previous experiments[15] by visualization with a video camera.

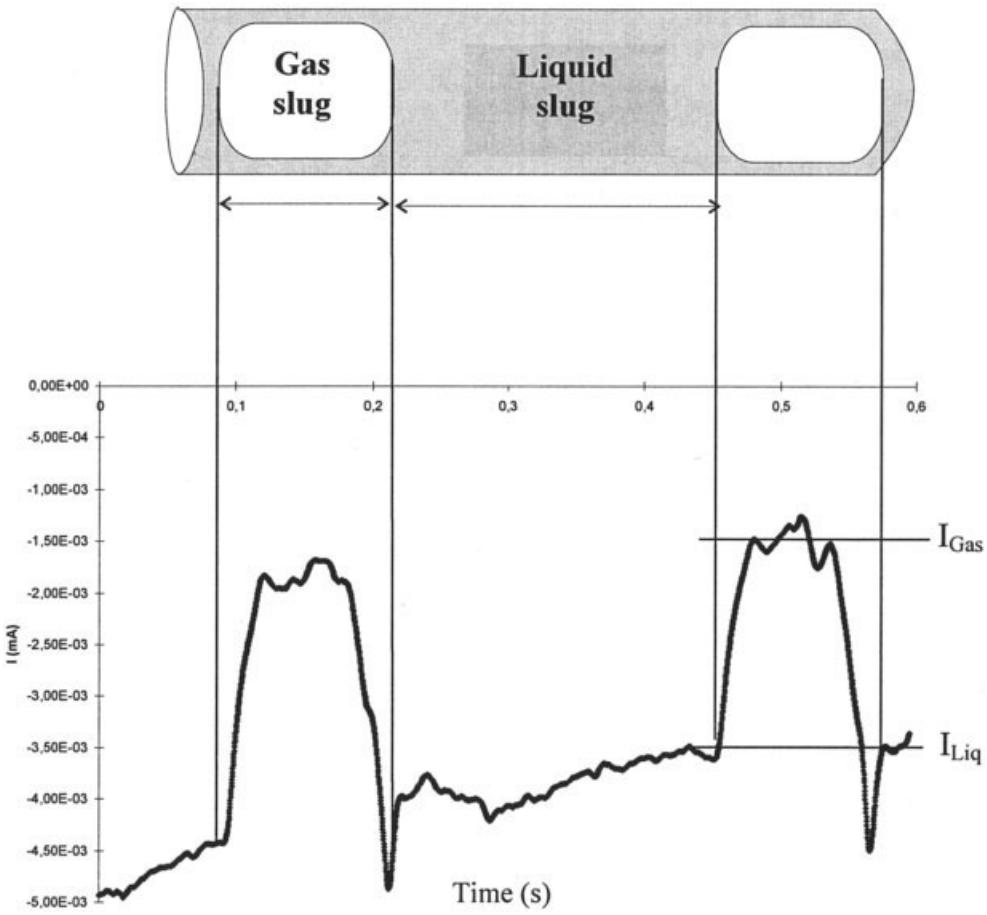

Figure 10. Electrochemical signal for passing air slugs.

The results obtained by the two methods can then be compared (Figure 12).

Values of gas slug frequency determined by visualization are very similar to those obtained by electrochemical measurements, thus providing additional validation of the electrochemical method.

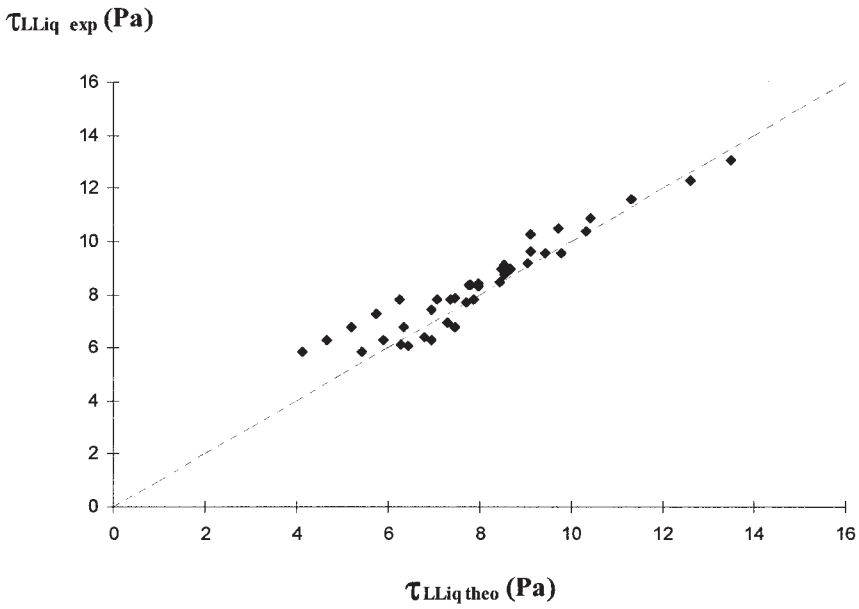

Figure 11. Experimental wall shear stress near liquid slugs vs. theoretical value.

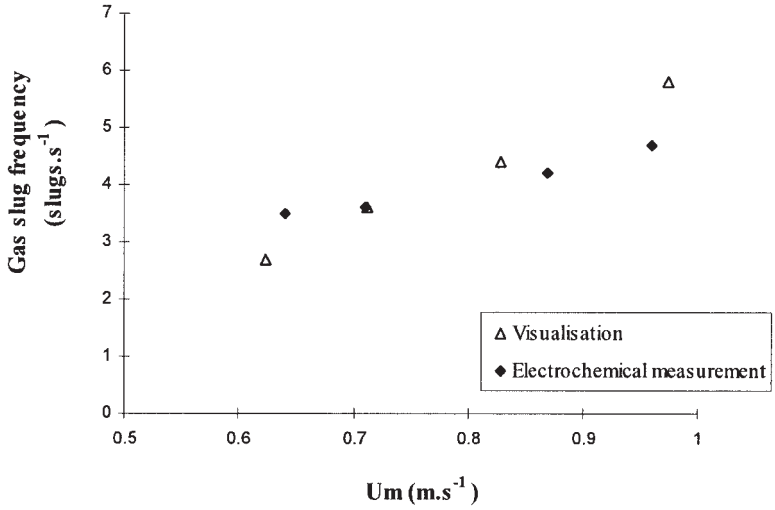

Figure 12. Gas slug frequency vs. U_m.
U_{Liq} = 0.5 m s^{-1}.

Wall Shear Stress Measurement in Gas Slugs. For each operating condition, the absolute value of I_{Gas} was used to calculate the experimental absolute value of the wall shear stress near the gas slug. Figure 13 represents the variation of this shear stress vs. the gas superficial velocity.

For a given value of U_{Liq}, the absolute value of τ_{LGas} increases with U_{Gas}, although this increase is relatively small. For instance, for U_{Liq} = 0.55 m s^{-1}, τ_{LGas} increases from 0.9 to 2.5 Pa when U_{Gas} increases from 0 to 1 m s^{-1}. τ_{LGas} also increases with U_{Liq} for a given value of U_{Gas}. For a liquid velocity of 0.87 m s^{-1}, the wall shear stress near gas slug becomes constant for a definite value of U_{Gas} (in that case equal to 0.7 m s^{-1}), although this behavior is not observed for the other values of the liquid superficial velocity. Shear stress near the gas slug is linked to both liquid and gas superficial velocity but its increasing rate is low. It is then possible to posit that its value is essentially linked to the liquid film thickness around the gas slugs. This will be discussed in the next section.

Comparison between Modeled and Measured Shear Stresses: Estimation of the Decreasing Liquid Film Thickness

With respect to the shear stresses near liquid slugs, the comparison between the two methods was discussed in the previous paragraph. The values obtained by the two methods have been shown to be very close, which confirms the validity of measurements.

Concerning the shear stresses near gas slugs, Figure 14 represents values of τ_{LGas} obtained by the two methods.

As mentioned earlier, the electrochemical method does not

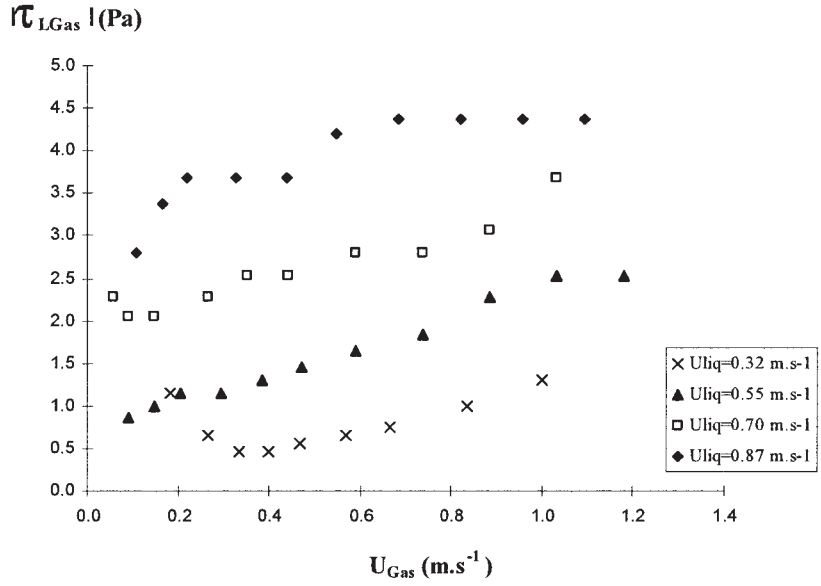

Figure 13. Absolute value of wall shear stress near gas slugs vs. U_{Gas} for different values of U_{Liq}.

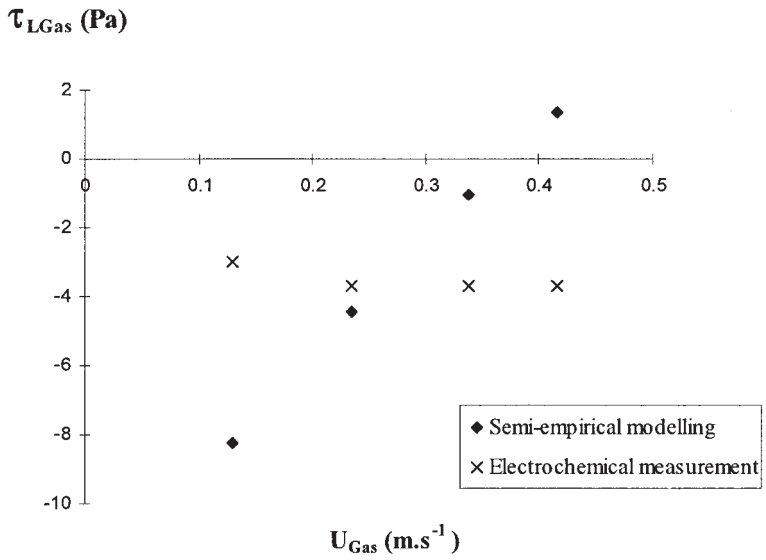

Figure 14. Wall shear stress near gas slugs vs. U_{Gas} by the two different approaches.

$U_{Liq} = 0.87$ m s^{-1}; $D = 1 \times 10^{-3}$ m.

allow us to know the sign of the shear stress. However, by analogy to previous works, the assumption will be done in the following part of the study that the liquid film surrounding the gas slugs is decreasing, and so the wall shear stress near gas slugs can be considered to be negative.

As demonstrated in Figure 14, the results obtained by the two methods are quite different. Computed values of wall shear stress near the gas slug are negative and relatively high in absolute value for a mean velocity < 1.2 m s^{-1}. When U_m increases, computed τ_{LGas} decreases in absolute value and becomes positive for a mean velocity > 1 m s^{-1}. On the contrary, measured wall shear stresses are low and vary very little with the mean velocity: the absolute value of τ_{LGas} increases slightly with the mean velocity U_m until a limit value corresponding to $U_{Gas} = 0.1$ m s^{-1}, after which it no longer seems to depend on U_m.

To understand why experimental shear stresses were low and almost unrelated with superficial velocities, the idea was to determine the film thickness near the gas slug.

Measured wall shear stresses will be considered as the most available. Indeed, on one hand, the methodology was validated for the one-phase flow and for the liquid slugs; and, on the other hand, the modeling leads to results that have no physical significance for low gas velocities.

Equations of the two-phase modeling (from 5 to 22) were used to calculate the film thickness e from different known parameters such as the air slug velocity V_s, gas superficial velocity U_{Gas}, liquid superficial velocity U_{Liq}, and the measured value of wall shear stress near gas slugs τ_{LGas}

$$e^2\tau_{LGas} - 2\mu_L V_s e + \mu_L r(V_s - U_{Gas} - U_{Liq}) = 0 \qquad (32)$$

Assuming that the wall shear stress near gas slugs is negative, only one root of this equation is physically possible

$$e = \frac{2\mu_L V_s - 2\sqrt{\mu_L^2 V_s^2 - \tau_{LGas}\mu_L r(V_s - U_{Gas} - U_{Liq})}}{2\tau_{LGas}} \qquad (33)$$

Table 2 presents the values of the film thickness calculated both by the Bretherton relationship (Eq. 25) and by the present method.

Computed values of e are in the same range as values obtained according to the Bretherton equation (see Table 2).

However, with the Bretherton equation, the film thickness increases with the gas superficial velocity (from 41 to 56 μm), whereas the values obtained from Eq. 33 do not seem to depend on this experimental parameter. This result may lead to the assumption that the film thickness is controlled more by the solid/liquid surface tension effect than by hydrodynamics.

The use of the Bretherton equation can be discussed because this correlation has been established for a gas slug moving in a motionless liquid, of which some conditions of flow are different from those reported in that study. It was then decided to use the two-phase model, taking into account our description of e instead of the Bretherton equation, and to compare values of wall shear stresses near gas slugs obtained by two methods: (1) measured by the electrochemical method and (2) obtained by modeling with recalculated values of e (Figure 15).

Obtained τ_{LGas} values were negative for both of the above approaches. Recalculated values of τ_{LGas} (method 2) are much closer to the measured τ_{LGas}.

However, there is still a difference between the values, of about 20%, which can be explained by the relative error made on the film thickness calculation. Moreover, the empirical

Table 2. Values of e Obtained by Two Different Approaches*

U_{Gas} (m s^{-1})	Values of e (Bretherton Relationship) (μm)	Values of e (This Method) (μm)
0.11	41	46
0.16	46	46
0.22	47	46
0.33	50	46
0.44	53	46
0.55	56	46

*$U_{Liq} = 0.87$ m s^{-1}.

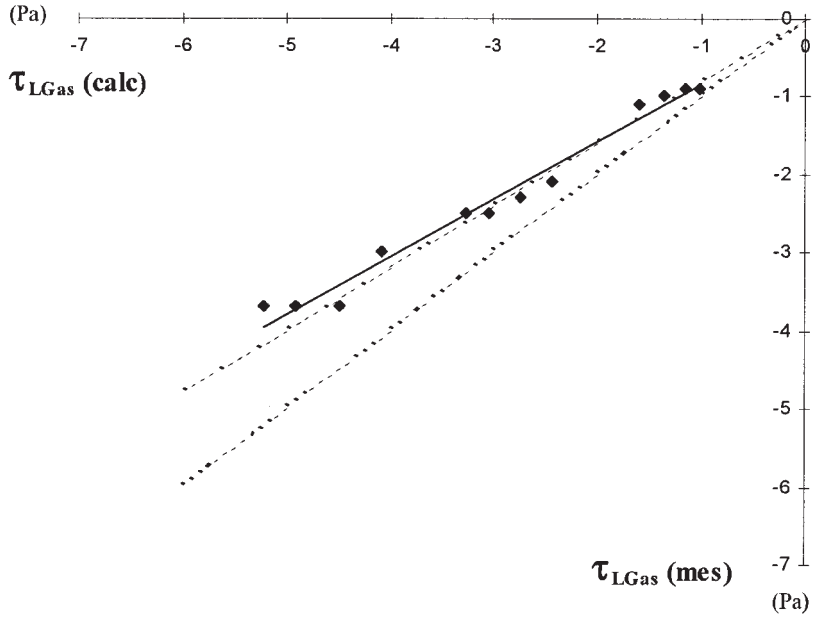

Figure 15. Computed wall shear stress near gas slugs vs. measured values.

$U_{Liq} = 0.87$ m s^{-1}; $D = 1 \times 10^{-3}$ m; U_{Gas} between 0.1 and 0.6 m s^{-1}.

relationship (Eq. 11) is used to calculate the air slug velocity V_s. This value of V_s is used many times in the model that can explain the gap between values of τ_{LGas} obtained by the two approaches.

The model describes the variation of τ_{LGas} vs. U_{Liq} and U_{Gas} but the absolute value of τ_{LGas} is underestimated by about 20%.

Conclusion

The aim of this study was to characterize wall shear stresses generated by a gas–liquid two-phase flow inside a capillary, following two approaches.

The first approach consisted in a calculation of these shear stresses by use of a two-phase model, including flow parameters that were determined experimentally in a previous study.[15] Moreover, the resolution of the set of equations needed the use of an equation drawn from the literature,[19] describing the film thickness around the gas slugs. The use of this equation, established for a gas slug moving in a motionless liquid, introduced a strong uncertainty into the calculation of the shear stresses by the two-phase model and induced some results having no physical signification in the case of low gas velocity.

The second approach constituted a direct and local measurement of wall shear stresses by an electrochemical method. This method presents technological difficulties, although it introduces few assumptions and elucidates a great deal of information about the flow (shear stress, slug length, frequency). Among them, the shear stress near the gas slugs, an unknown parameter until then, was obtained for different operating conditions. Moreover, a calculation of the liquid film thickness around the gas slugs from measured values of the shear stresses verified that this thickness does not depend on gas velocity. It may be possible that the film thickness is controlled more by the solid/liquid surface tension effect than by hydrodynamics.

Acknowledgments

The authors thank R. Ascione and Pr. A. Liné for their contribution to this study.

Notation

Ca = capillary number
d = probe diameter, m
D = capillary inner diameter, m
D_f = diffusivity coefficient, m^2 s^{-1}
D_{Gas} = hydraulic diameter near the gas slug, m
D_{Liq} = hydraulic diameter near the liquid slug, m
e = liquid film thickness, m
f = friction factor
f_{Gas} = friction factor near the gas slug
f_{Liq} = friction factor near the liquid slug
i = diffusion limit current, A
I_{Gas} = intensity near the gas slug, A
I_{Liq} = intensity near the liquid slug, A
Q_{Gas} = gas flow rate, m^3 s^{-1}
Q_{Liq} = liquid flow rate, m^3 s^{-1}
r = capillary radius, m
Re_{Gas} = Reynolds number characterizing the liquid flow near the gas slugs
Re_{Liq} = Reynolds number characterizing the liquid flow in the liquid slugs
R_G = gas holdup
R_L = liquid holdup
R_{LGas} = liquid holdup in the gas slugs
R_{LLiq} = liquid holdup in the liquid slugs
S = local velocity gradient, s^{-1}
U_{Gas} = gas superficial velocity for a two-phase flow, m s^{-1}
U_{Liq} = liquid superficial velocity for a two-phase flow, m s^{-1}
U_L = mean liquid velocity for a one-phase flow, m s^{-1}
U_{LGas} = liquid velocity near the gas slug, m s^{-1}
U_{LLiq} = liquid velocity near the liquid slug, m s^{-1}
U_m = mean velocity of the flow, m s^{-1}
V = total volume of the dispersion (gas + liquid), m^2
V^G = volume of the gas phase, m^2
V_s = gas slug velocity, m s^{-1}

Greek letters

ε_i = air injection ratio
Φ_{Liq} = liquid flux between a gas slug and a liquid slug, m s^{-1}
Φ_{Gas} = gas flux between a gas slug and a liquid slug, m s^{-1}
μ_L = liquid viscosity, Pa·s
ρ_L = liquid density, kg m^{-3}
σ_L = surface tension, N m^{-1}
τ_{LLiq} = wall shear stress generated by the liquid slug, Pa
τ_{LGas} = wall shear stress generated by the liquid film near the gas slug, Pa
τ_{theo} = theoretical wall shear stress generated by the one-phase flow, Pa
τ_{exp} = experimental wall shear stress measured for the one-phase flow, Pa

Literature Cited

1. Futselaar H. Flexible system design and process operation for water treatment systems. Proc of the Conf on Membranes in Drinking and Industrial Water Production, Paris, France; 2000;2:335-343.
2. Verberk JQJC, Worm GIM, Futselaar H, Van Dijk JC. Combined air–water flush in dead-end ultrafiltration. Proc of the Conf on Membranes in Drinking and Industrial Water Production, Paris, France; 2000;2:655-663.
3. Cui ZF, Wright KIT. Gas–liquid two-phase cross-flow ultrafiltration of BSA and dextran solutions. *J Membr Sci*. 1994;90:183-189.
4. Mercier M, Fonade C, Lafforgue-Delorme C. How slug flow can enhance the ultrafiltration flux in mineral tubular membranes. *J Membr Sci*. 1997;128:103-113.
5. Vera L, Villarroel R, Delgado S, Elmaleh S. Enhancing microfiltration through an inorganic tubular membrane by gas sparging. *J Membr Sci*. 2000;165:47-57.
6. Bellara SR, Cui ZF, Pepper DS. Gas sparging to enhance permeate flux in ultrafiltration using hollow fibre membranes. *J Membr Sci*. 1996; 121:175-184.
7. Cabassud C, Laborie S, Lainé JM. How slug flow can enhance the ultrafiltration flux in organic hollow fibres. *J Membr Sci*. 1997;128: 93-101.
8. Laborie S, Cabassud C, Durand-Bourlier L, Lainé JM. Flux enhancement by a continuous tangential gas flow in ultrafiltration hollow fibres for drinking water production : Effects of slug flow on cake structure. *Filtr Sep*. 1997;34:887-891.
9. Ducom G, Matamoros H, Cabassud C. Air sparging for flux enhancement in nanofiltration membranes: Application to O/W stabilised and non-stabilised emulsions. *J Membr Sci*. 2002;204:221-236.
10. Cabassud C, Laborie S, Durand-Bourlier L, Lainé JM. Air sparging in ultrafiltration hollow fibers: Relationship between flux enhancement, cake characteristics and hydrodynamic parameters. *J Membr Sci*. 2001; 181:57-69.
11. Ducom G, Puech FP, Cabassud C. Air sparging with flat sheet nanofiltration: A link between wall shear stresses and flux enhancement. *Desalination* 2002;145:97-102.
12. Mercier-Bonin M, Maranges C, Lafforgue C, Fonade C, Liné A. Hydrodynamics of slug flow applied to cross-flow filtration in narrow tubes. *AIChE J*. 2000;46:476-488.
13. Bendiksen KH. An experimental investigation of the motion of long bubbles in inclined tubes. *Int J Multiphase Flow*. 1984;10:467-483.
14. Collins R. The motion of large bubbles rising through liquid flowing in a tube. *J Fluid Mech*. 1978;89:497-514.
15. Laborie S, Cabassud C, Durand-Bourlier L, Lainé JM. Characterisation of gas–liquid two-phase flow inside capillaries. *Chem Eng Sci*. 1999;54:5723-5735.
16. Fabre J, Liné A. Slug flow modelling. *International Encyclopedia of Heat and Mass Transfer*, Brooklyn, NY: Innodata Corp.; 1996:1015-1021.
17. Fairbrother F, Stubbs AE. Studies in electroendosmosis—VI. The "bubble tube " method of measurement. *J Chem Soc*. 1935;1:527-529.
18. Marchesssault RN, Mason SG. Flow of entrapped bubbles through a capillary. *Ind Eng Chem*. 1960;52:79-84.
19. Bretherton FP. The motion of long bubbles in tubes. *J Fluid Mech*. 1961;10:166-188.
20. Schwartz LW, Princen HM, Kiss AD. On the motion of bubbles in capillary tubes. *J Fluid Mech*. 1986;172:259-275.
21. Reiss L, Hanratty T. Measurement of instantaneous rates of mass transfer to a small sink on a wall. *AIChE J*. 1962;8:245-247.
22. Reiss L, Hanratty T. An experimental study of the unsteady nature of the viscous sublayer. *AIChE J*. 1963;9:154-158.
23. Cognet G. *Contribution à l'Étude de l'Écoulement de Couette par la Méthode Polarographique*. Thèse d'Etat. Nancy, France: Université Nancy; 1968.
24. Koeck C. *Etude du Frottement Pariétal dans un Écoulement Diphasique Vertical Ascendant*. Thèse de doctorat. Paris, France: Paris VI Université; 1980.
25. Cognet G, Lebouché M, Souhar M. Wall shear measurements by electrochemical probe for gas–liquid two-phase flow in vertical duct. *AIChE J*. 1984;30:338-341.
26. Galier S, Issanchou S, Moulin P, Clifton M, Aptel P. Electrochemical measurement of velocity gradient at the wall of a helical tube. *AIChE J*. 2003;49:1972-1979.
27. Gaucher C, Jaouen P, Comiti J, Legentilhomme P. Determination of cake thickness and porosity during cross-flow ultrafiltration on a plane ceramic membrane surface using an electrochemical method. *J Membr Sci*. 2002;210:245-258.
28. Storck A, Coeuret F. *Eléments de Génie Électrochimique*. Paris, France: Lavoisier Tec & Doc (VCH Publishers); 1984.

Manuscript received Apr. 28, 2004, and revision received Aug. 13, 2004.